Assessment of long-term offshore wind energy potential in the south and southeast coasts of China based on a 55-year dataset

Yi Wen[1], Bahareh Kamranzad [2,3], Pengzhi Lin[1*]

[1] State Key Laboratory of Hydraulics and Mountain River Engineering, Sichuan University, 24, South Section No.1, Yihuan Road, Chengdu, P. R. China 610065

[2] Graduate School of Advanced Integrated Studies in Human Survivability (GSAIS), Kyoto University, Yoshida-Nakaadachi 1, Sakyo-ku, Kyoto 606-8306, Japan

[3] Hakubi Center for Advanced Research, Kyoto University, Yoshida Honmachi, Sakyo-ku, 606-8501, Kyoto, Japan

* corresponding author's email: cvelinpz@126.com

Abstract

Offshore wind energy resources assessment is necessary for safe, efficient, and reasonable development and utilization of the resources. In this study, based on the 55-yearly wind reanalysis dataset of the JRA-55 model developed by the Japan Meteorological Agency (JMA), the Spatio-temporal variation of wind energy potential, as well as rates of change in the whole period were assessed in the South China Sea. Furthermore, a methodology to determine the most suitable location and wind turbine of offshore wind energy extraction based on different factors including long-term change and wave condition on the south coast of China was proposed. The results showed that the Luzon strait and Taiwan strait showed higher wind energy potential. However, the intra-annual fluctuation of the wind resources is significantly high in Luzon Strait, ranging from 400 to 2500 W/m^2. The investigation of long-term changes showed that most of the South China Sea experienced a remarkable decrease in the second decade (1971-1980), but the overall long-term wind energy trend during five decades was mostly neutral. The investigation in the selected points indicated that the most suitable location and wind turbines are the nearshore of Quanzhou, Fujian and SWT-7.0-154, respectively. The suggestions for future offshore wind power development should be the coasts of Hong Kong

This is a peer-reviewed, accepted author manuscript of the following article: Wen, Y., Kamranzad, B., & Lin, P. (2021). Assessment of long-term offshore wind energy potential in the south and southeast coasts of China based on a 55-year dataset. Energy, [120225]. https://doi.org/10.1016/j.energy.2021.120225

considering that there have been wind farms under construction in Fujian, and there are promising potential to generate 35.36 MWh per year per wind turbine in the coasts of Hong Kong.

Keywords: Offshore wind resources; South China Sea; Sustainability; Spatio-temporal variation; Long-term change

1. Introduction

In today's world, where coal, oil, and other conventional energy are increasingly scarce, energy bottleneck has become a critical problem restricting the sustainable development of various countries. Many countries, including China, generally advocate the application of clean energy, energy conservation, and emission reduction, to effectively deal with the increasingly severe resource and environmental crisis.

As the delegate for the new and green marine energy, offshore wind energy has grown on the explosive type in the recent decade. Europe is the largest region for offshore wind farms installations, where the cumulative offshore wind power capacity in UK reached 8480MW until 2019, reinforcing its leadership position in the world. Following closely, is Germany (7372MW) (WINDPOWER). Moreover, advantages such as more significant suitable free areas, low visual and sound impact, and the higher energy potential in comparison with the onshore, favor the development of offshore wind farms (Esteban et al., 2011; Sant'Anna de Sousa Gomes et al., 2019; He et al., 2020).

Offshore wind energy resources have been assessed from global to local. The potential of global offshore wind energy resources have been evaluated and classified based on 37-yearly ERA-40 database (Zheng et al., 2018). Sant'Anna de Sousa Gomes et al.(2019) proposed a method to evaluate and utilize wind energy along the southeastern coast of Brazil using one year dataset. Costoya et al.(2020) analyzed the current offshore wind resources using a 30-year historical datasatand predicted the future changes, as the U.S. offshore wind sector is expected to have an important development in the next decade. The Analytic Hierarchy Process (AHP) was used to detect the most suitable offshore wind energy installation area in Turkey based on

multiple evaluation criteria including …… (Emeksiz and Demirci, 2019). Kim et al. (2013) evaluated the offshore wind resource around the Korean Peninsula and detected the most suitable installation location around the candidate coasts using a 3-year dataset.

China, being exposed to the East and South China Sea, is capable of providing parts of its energy demand from marine resources, especially from offshore wind energy. Although China has the largest installed capacity of wind energy globally, offshore wind energy only accounts for 2% (WINDPOWER, n.d.). There are many offshore wind farms under construction in China, such as Jiangsu, Shanghai, Guangdong, Fujian, etc. But China's rapid economic expansion requires new areas of innovation, learning, and improvement to accelerate offshore wind deployment (Renewables Consulting Group, 2020). Wind resources, including onshore and offshore, have been investigated in several previous types of research (e.g., Dong et al., 2019; Wan et al., 2018; Wang et al., 2018). Nie & Li (2018) discussed offshore wind energy potential along the China coast using statistical methods such as….. Hong and Möller (2011) investigated the offshore wind energy resources in China's Exclusive Economic Zone (EEZ) using Geographic Information Systems (GIS). He et al. (2020) assessed offshore wind energy potential in Hong Kong based on a high-resolution Numerical Weather Prediction (NWP) model in conjunction with observations. Wu et al. (2020) proposed a decision framework to apply for offshore wind power station selection in China, in which an evaluation system was proposed considering both exclusion index and evaluation index.

In the above studies, wave condition and long-term changes in offshore wind sources have not been taken into account in selecting suitable sites. Wave condition should be an important consideration in the survival of wind turbines in extreme condition and operation and maintenance of wind turbines. Besides, long-term changes should be investigated considering the sustainable development of wind resources. Hence, this study aims to identify the most suitable wind turbine installation location in the South China Sea, considering both wave condition and long-term variations in wind resources. For this purpose, a 55-yearly wind re-analysis by JRA-55 model will be used to assess the sustainability of offshore wind resources in the South China Sea to provide the necessary results for the designation of suitable wind energy extraction locations. A method will be proposed to detect the most suitable location for

wind turbines installation considering energy potential (wind power density, capacity factor, and rich level occurrence), stability (Monthly Variability Index (MVI) and Coefficient of Variation (CV)), Rate of Change (RoC), extreme condition (99th percentile wind speed and 99th percentile wave height), accessibility, distance to coast and water depth, for the first time.

In this paper, data and methods, including data source and all assessment criteria, will be introduced in section 2. section 3 contains the results and discussion, including Spatio-temporal variations and long-term change and selection of suitable locations and wind turbines based on different criteria. Section 4 summarizes the results and discussion.

2. Data and methods

2.1. Data sources

The JRA-55 wind reanalysis dataset hosted at Japan Meteorological Agency (JMA) (KOBAYASHI et al., 2015) is used to assess the offshore wind resource in the South China Sea. Its temporal and spatial resolutions are 6 hr and 60 km, respectively. It covers the time range from January 1958 to December 2012, with a spatial coverage of 105.5°E-123.5°E and 17°N - 30°N (Fig. 1).

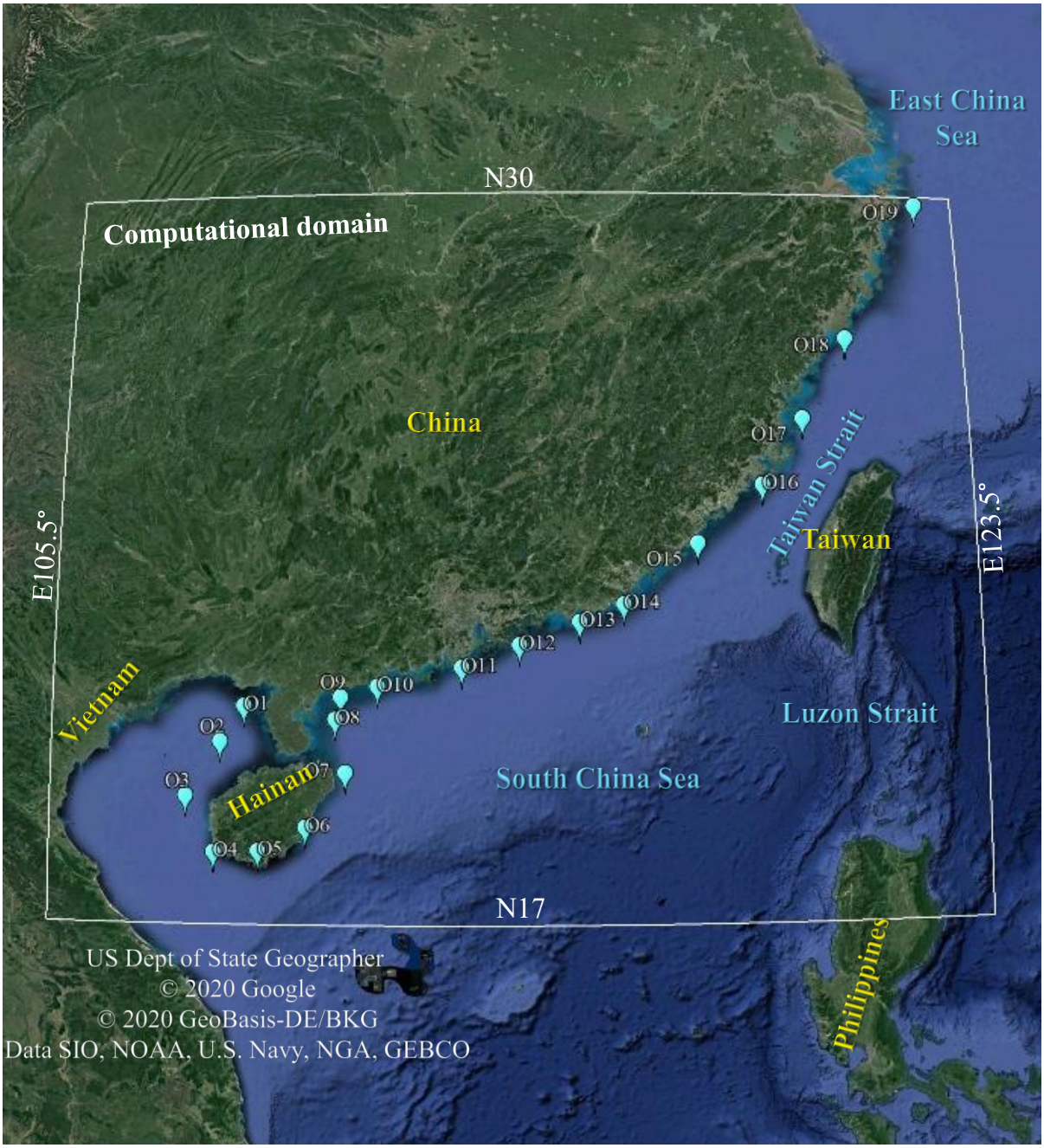

Fig. 1. Study area and the location of selected sites

2.2. Methods

2.2.1 Energy potential

The JRA-55 wind reanalysis dataset obtained the wind field at 10 m above the sea surface for the past 55 years (1958-2012). Many wind sources have been assessed at 10 m above the sea surface in the previous studies (e.g., Wan et al., 2018; Zheng et al., 2013; Zheng et al., 2018;

Dong et al., 2019). However, the hub height of wind turbines is generally considered to be between 70 and 100 m for wind energy studies (Silva et al., 2016; Sant'Anna de Sousa Gomes et al., 2019). Hence, in this study, the height of 100 m is selected for assessing the wind energy. The wind speed at different heights can be calculated as follow (Hsu, 1994):

$$U = U_r \left(\frac{Z}{Z_r}\right)^{\alpha} \quad (1.)$$

where U is the wind speed at Z, U_r is the wind speed at reference height Z_r, and α is the wind shear exponent, which is related to atmospheric stability and surface roughness. $\alpha = 0.11$ is generally suggested to use at sea (Hsu, 1994) He et al., 2020; Shu et al., 2015). Hence, 0.11 is adopted as a wind shear exponent in this study.

The Wind Power Density (WPD) is used to assess the wind energy resource, and it is calculated as follow (Silva et al., 2016):

$$WPD = \frac{1}{2}\rho \cdot V^3 \quad (2.)$$

where ρ is the air density (1.225 kg/m^3 in this study) and V is the wind speed at hub height.

The Energy Production (P_t) and Capacity Factor (CF) of a wind turbine can be used to investigate the actual energy output, which is shown as follows (Sant'Anna de Sousa Gomes et al., 2019):

$$P_t = \frac{1}{2}\rho \cdot C_P \cdot A_T \cdot V^3 \quad (3.)$$

$$CF = \frac{\overline{P_t}}{P_e} \quad (4.)$$

where C_P is the turbine capacity, 0.4 can be adopted for modern wind turbines (Sant'Anna de Sousa Gomes et al., 2019). A_T and P_e are swept area of blade and rating power, respectively, and they can be checked in the technical catalog of the wind turbines manufacturer. In addition, $\overline{P_t}$ is the average annual energy production.

The Rich Level Occurrence (RLO) which is the occurrence of WPD greater than 200W/m^2, indicates the richness of wind energy (Zheng et al., 2018). Generally, larger RLO values show larger wind energy potential.

2.2.2 Intra-annual variability

Energy stability must be considered in wind energy assessment since it is closely related to the collection, conversion efficiency and the life of the wind turbines. Coefficient of Variation (CV) mainly reflects the resource volatility within a monthly scale. As a negative indicator, lower values of CV show higher stability of wind energy. It can be calculated as follows:

$$CV = \frac{\sigma_P}{\bar{P}} \tag{5.}$$

in which, σ_V is the standard deviation and $\bar{V}$ is the mean value of wind power density.

Monthly Variation Index (MVI) can be considered a good approximation in assessing the intra-annual variation of the resources. It can be calculated as follows (Zheng et al., 2013):

$$MVI = \frac{P_{M1} - P_{M12}}{P_{year}} \tag{6.}$$

where P_{M1} and P_{M12} are the highest and lowest monthly means of wind power density, respectively, while P_{year} is the annual average wind power density.

2.2.3 Rate of change

Rate of change is used to assess the stability of wind resources in long-term for medium and long-term planning of resource development and prediction. Therefore, the rate of change in five decades and decade will be discussed using time series of wind power density and they will be calculated as the slope of the best fitting line between the 55 years mean values of each grid point.

2.2.4 Extreme condition

Another important consideration for offshore structures is the device survivability in extreme conditions. Since 2007, more than 100 wind turbines' accidents have occurred each year, and 326 failure accidents have occurred from 2012 to 2013. Previous studies have shown that 52.2%

of large wind turbine tower collapses are caused by strong winds and storms(Chou and Tu, 2011). For example, in 2008, a strong typhoon "Jangmi" struck Taiwan and caused the collapse of No. 2 wind turbine on the shore of Taichung Harbor(Chou and Tu, 2011). The extreme wind speed has been considered in the previous studies (Zheng et al., 2018; Costoya et al., 2020). However, for offshore wind farms, the marine environment of wind turbines is much more complex than that of onshore. the estimation of extreme wave height is essential for piling system, coastal structure size determination and reinforcement for wind turbines (Lavidas, 2020). In this study, the extreme values of both wind and wave will be considered as essential factors for construction cost for wind turbines, and they will be estimated using the 99^{th} percentage of the time series of wind speed and wave height for 55 years. The time series of wave height is from our previous study (Kamranzad et al., 2020).

2.2.5 Accessibility

Accessibility is a crucial characteristic for offshore wind farms in operation and maintenance (O&M), and it requires long enough time slots to ensure that sea conditions are suitable and safe for crew and vessel deployment (Gallagher et al., 2016). When the ocean parameters (significant wave height, wind speed and peak period) is equal to or less than the certain thresholds, the percentage of time is called accessibility, and the thresholds depend on the type of the employed vessel (O'Connor et al., 2013). In this study, the thresholds of 13 s for the peak period, 2 m for significant wave height and 16 m/s for wind speed is adopted, as suggested by Gallagher et al. (2016).

2.2.6 Distance to coast and water depth

Water depth and distance to coast are among the most critical consideration in the installment of offshore wind turbines. Low water depth and short distance to coast can reduce the cost in transporting power to the land. The increase of depth and distance in areas considered for the development for offshore wind farms indicates the increases the establishment costs of anchorage, cabling and piling (Costoya et al., 2020). Generally, offshore wind turbines are

installed below 60 m (Aymen Chaouachib, Catalin Felix Covriga,∗, 2017; Emeksiz and Demirci, 2019). Therefore, areas with water depths less than 60 m and distances to coast less than 50 Km were selected in the study.

2.2.7 A novel suggested approach for determining the most suitable location

A multi-criteria approach for determining the most suitable location will be proposed considering the WPD, CF, RLO, CV, MVI, OM, EWS, EWH, RC, DC and WD. All factors will be normalized and then given different weights. The standardization method is as follows:

For positive factors:

$$y_i = \frac{x_i}{\max(x_i)} \tag{7.}$$

For negative factors:

$$y_i = \frac{\min(x_i)}{x_i} \tag{8.}$$

where x_i is the initial value and y_i is the value after being normalized. All values of both positive factors and negative factors are between 0 and 1 after being normalized, and a higher value indicates better suitability for all factors. The weights are given according to the previous research (Zheng et al., 2018; Costoya et al., 2020), and more factors, such as extreme wave height, rate of change and accessibility, are considered. The multi-criteria approach is shown as follows:

$$\begin{aligned} \mathrm{F} = {} & 0.177 * \mathrm{WPD} + 0.176 * \mathrm{CF} + 0.082 * \mathrm{RLO} + 0.077 * \mathrm{CV} + 0.038 * \mathrm{MV} + 0.058 * \mathrm{EWS} \\ & + 0.058 * \mathrm{EWH} + 0.008 * \mathrm{ROC} + 0.081 * \mathrm{OM} + 0.053 * \mathrm{WD} + 0.12 * \mathrm{DC} \end{aligned} \tag{9.}$$

where F is the expectation value, and a higher value indicates higher suitability in the site.

3. Results and discussion

3.1 Spatio-temporal analysis of wind speed and wind power density

The spatial distribution of the annual average wind speed and wind power density at 100m in the South China Sea are shown in Fig. 2. As shown in Fig. 2, the area with the particularly high

wind resource is mainly Taiwan Strait, where WPD is above 1200W/m^2 and annual average wind speed reaches around 15m/s, closely followed is nearshore northern of Luzon Strait. The area with the lowest wind resource is south of Beibu Gulf. The dominant wind direction in the South China Sea is from the southeast, while in southern of Taiwan Strait it is from the east. Nie & Li. (2018) and Wan et al. (2018) showed the similar spatial distribution for wind resource in the domain, based on 28 and 38 years of wind dataset, respectively. And the result shows a similar spatial distribution and annual mean wind power density with Hong & Möller. (2011) in nearshore southern coasts of China.

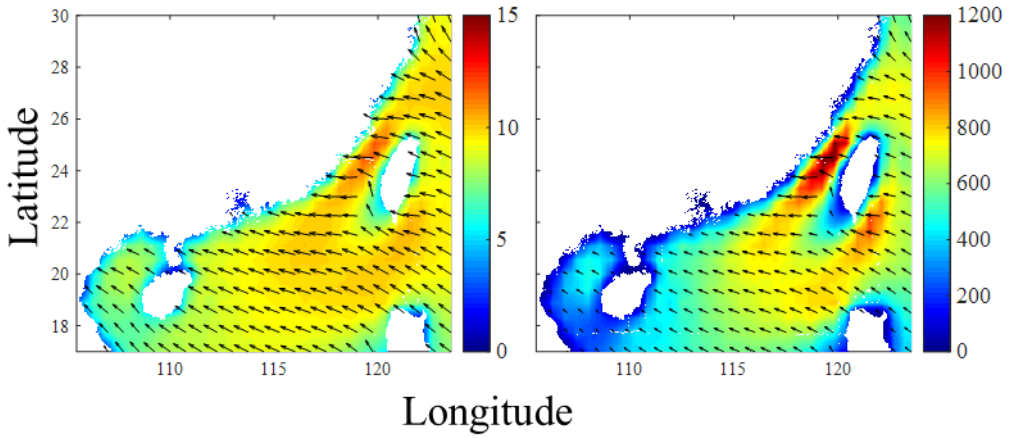

Fig. 2. The spatial distribution of the annual average wind speed (m/s) (left) and wind power density (W/m^2) (right) at 100 m

The intra-annual variability of wind characteristics and wind power density are calculated in the South China Sea and shown in Figs. 3 and 4, respectively. Fig. 3 presents the spatial distribution of the monthly mean of wind fields. The wind speed reaches the maximum (>15m/s) in December and November and the minimum in May. Fig. 4 represents the spatial distribution of the monthly mean values of wind power density, and it is similar to Fig. 3. According to this figure, the wind power density increases from May to reach the highest values (>2000W/m^2) in November and December and then, decreases until the lowest occurs in May. The result is consistent with results of Wang et al. (2018) in the domain. Furthermore, from November to January (winter), wind resources are significantly abundant in Taiwan Strait,

Luzon Strait and the central South China Sea. However, the intra-annual variation seems to be high in Luzon Strait and central South China Sea with the mean monthly wind power density fluctuating between 400 and 2500 W/m^2.

The South China Sea lies on the monsoon belt, and the wind direction changes with the seasons. The wind mainly blows from the east and northeast during Spring (March to May). Affected by the southwest monsoon, the wind direction of the whole South China Sea is mainly south during Summer (June to August), while the north of the Taiwan Strait is dominated by southeast wind. Autumn (September to November) is the monsoon changing season. From September to November, the main wind direction in the central and northern South China Sea has changed to northeast from southwest. Most of the South China Sea is dominated by the northeast wind in Winter (December to January), which is affected by the northeast trade wind (Wang et al., 2020). Furthermore, the maximum wind speed is located in Taiwan Strait, reaching above 15 m/s.

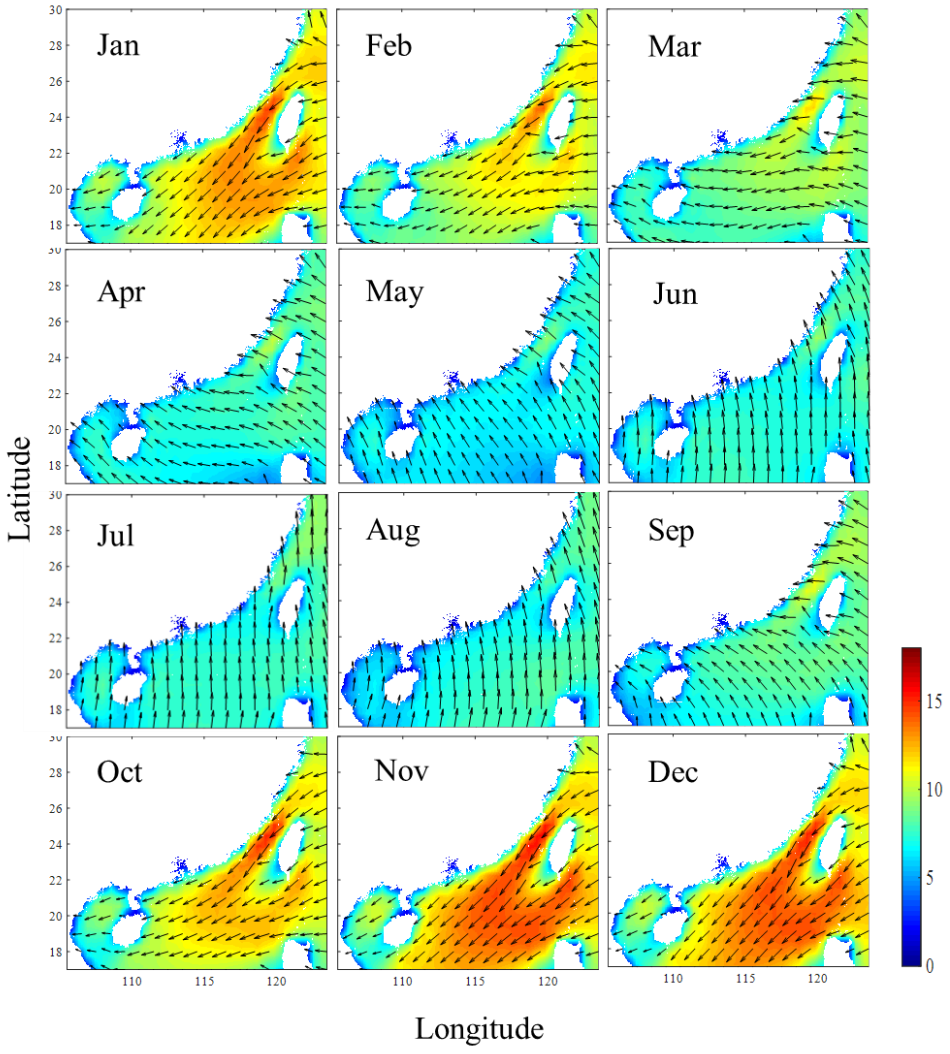

Fig. 3. The spatial distribution of the monthly average wind speed (m/s) at 100 m

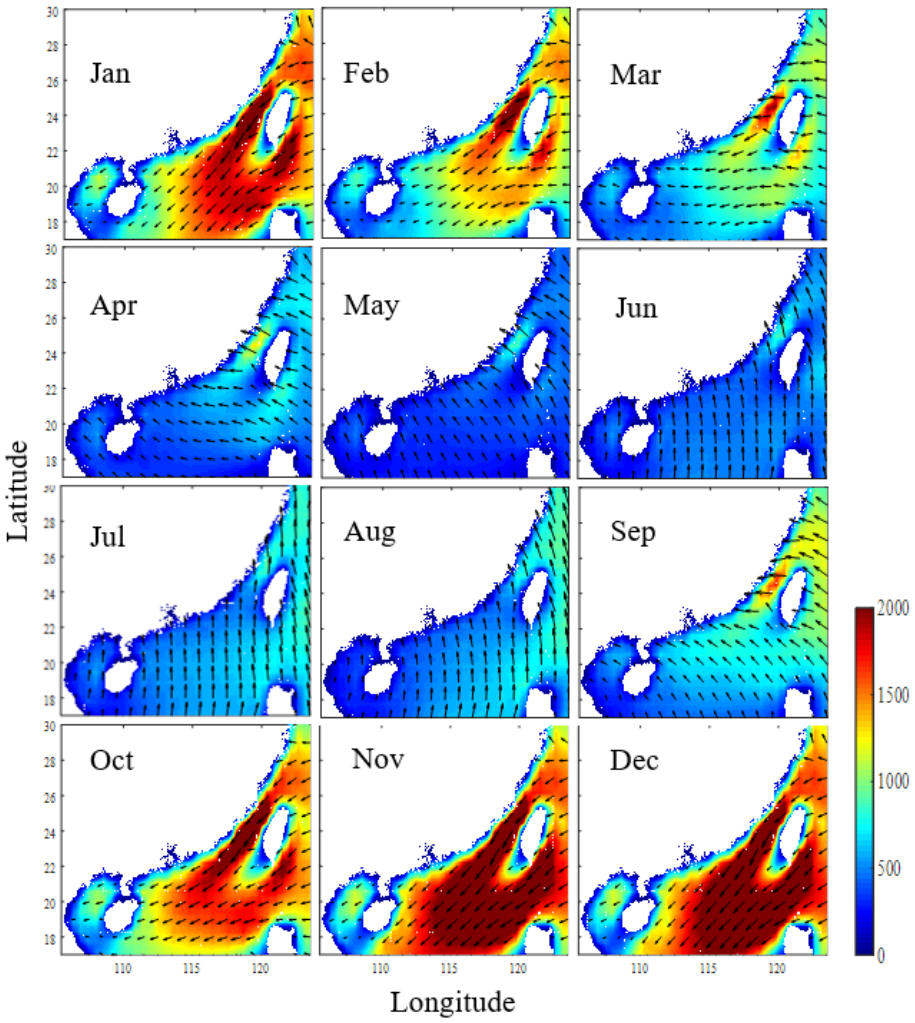

Fig. 4. The spatial distribution of the monthly wind power density (W/m^2) at 100 m

3.2 Intra-annual variability of wind resource

The suitable areas for planning the development of offshore wind farms are the ones with higher potential and lower variability(Astariz and Iglesias, 2016). The CV and MVI of wind power density are calculated to access the stability of offshore wind resource. Fig. 5 shows the spatial distribution of MVI (left) and CV (right) for the wind power density. According to Figure 5, Beibu Gulf and northern Taiwan show relatively low values of both MVI and CV. The central parts of South China Sea, except Beibu Gulf, exhibit higher variability of wind resource within monthly scale (MVI), whereas experience a high stability at the monthly scale (CV). The low stability of wind resource in monthly scale (MVI) in southern of South China

Sea is mostly affected by the southwest monsoon.

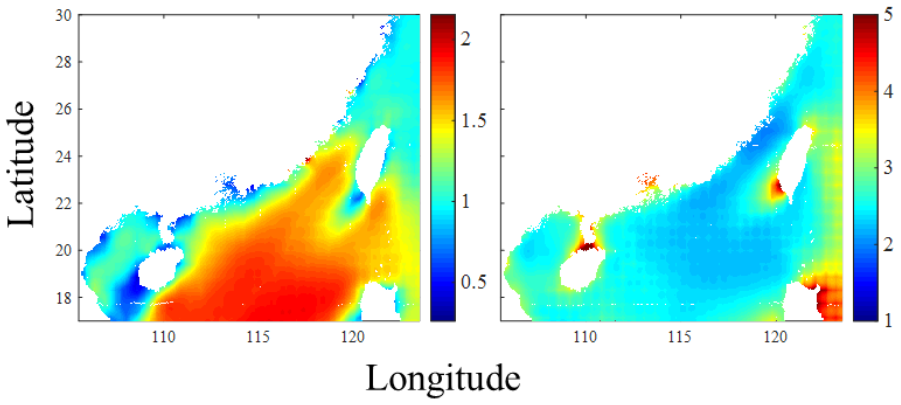

Fig. 5. MVI (left) and CV (right) for wind power density (W/m^2) at 100 m

3.3 Long-term change of wind resource

In order to assess the long-term change, five decades (from 1961 and 2010) of the offshore wind resources in the South China Sea are analyzed. The rate of change in five decades are used to discuss the long-term change and assess the sustainability of wind resources in long-term. Fig. 6 (a) shows the spatial distribution of the rate of change for wind power density in five decades. This figure shows no considerable decrease around Hainan, and a slight increase in the central parts of South China Sea. In general, there is no noticeable change in the majority of the domain except for a decrease in Taiwan Strait.

Decadal changes are investigated to evaluate the stability of the wind field in shorter periods and whether it is stable throughout the whole period (Kamranzad et al., 2020) and shown in Fig. 6 (b-f). According to Fig. 6 (b-f), the wind power density in most of the South China Sea increases slightly during the third (1981-1990) and fifth (2001-2010) decades. In contrast, over the second decade (1971-1980), a remarkable reduction of the wind power density can be observed. While the overall long-term wind trend observed is unremarkable in Taiwan Strait, a considerable increase of the wind energy resources is detected in the first (1961-1970) decade, and a substantial decrease in the second(1971-1980) decade and fourth (1991-2000) decade.

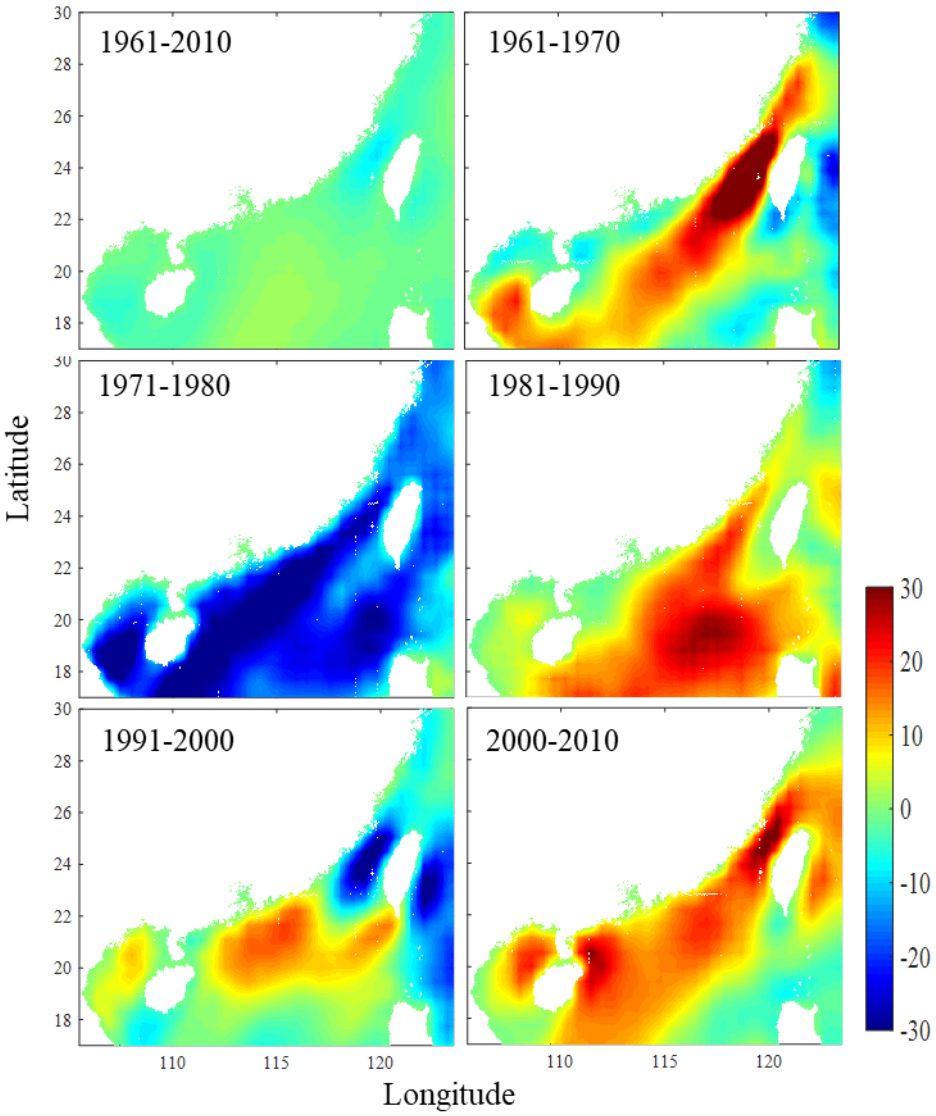

Fig. 6. Annual rate of change – 50-yearly (a) and 10-yearly (b-f)

3.4 Quantitative analysis

To determine the most suitable wind turbines and installation location, 19 sites were selected in the nearshore areas of the South China Sea. The points were selected in areas with water depth less than 60 m, and distance to coast less than 50 Km, as well as being located outside Taiwan Banks due to the giant sand wave fields (Zhou et al., 2018). Table 1 and Fig. 1 present the characteristics and locations of the selected sites . Table 1 indicates that the sites with the

highest wind speed is O16 and the lowest wind speed is presented at O6.

Table 1. Characteristics and locations of the selected sites

Point ID	Lat	Long	Depth (m)	Annual average wind speed at 100 m (m/s)	Distance from coast (km)
O1	20.7	109.25	20	6.95	48
O2	20.05	108.8	54	7.38	47
O3	19.05	108.15	39.5	7.45	49.2
O4	18.05	108.7	55	6.65	45.5
O5	18.1	109.55	56.8	6.76	7
O6	18.55	110.45	57.2	5.70	12.8
O7	19.55	111.2	56	7.42	19.5
O8	20.5	111	30	7.44	49.8
O9	20.9	111.1	30	7.19	48.3
O10	21.1	111.8	40	7.94	48.8
O11	21.45	113.4	45.5	8.42	49
O12	21.85	114.5	55.2	8.29	47
O13	22.25	115.65	57.7	8.98	46.5
O14	22.55	116.5	46.2	8.75	49.5
O15	23.6	117.95	29.2	8.55	47.5
O16	24.6	119.25	58.2	10.86	41.7
O17	25.75	120.1	41.5	9.63	49.4
O18	27.15	121.05	36	8.77	46.6
O19	29.5	122.7	46.5	9.40	46.1

In this study, 12 wind turbines with different characteristics and from different manufacturers are selected (https://en.wind-turbine-models.com/turbines). The output power of the wind turbine is determined by cut-in wind speed, cut-out wind speed and blade radius. Table 2 presents the main characteristics of each considered wind turbine, and Fig. 7 shows the power curve of each considered wind turbine. The power curve of a typical wind turbine is a graph that shows how much electrical power the turbine has at different wind

speeds(Karamichailidou et al., 2020). The highest output power observed in Fig. 7 is from the AMSC wt10000dd SeaTitan, and the rating wind speed ranges between 10 and 13 m/s for most of wind turbines.

Table 2. Wind turbines used in this study as adapted

Wind turbines	Rated power（MW）	Rotor diameter(m)	Cut-in wind speed (m/s)	Cut-out wind speed(m/s)
V100-2.0	2.0	100	3	22
V90-3.0	3.0	90	3.5	25
SWT-2.3-93	2.3	93	4	25
SWT-3.6-120	3.6	120	3.5	25
SWT-4.0-130	4.0	130	5	25
SWT-7.0-154	7.0	154	3	25
REpower5M	5.075	126.5	3.5	30
REpower6M	6.15	126	3.5	30
Nordex N90/2500	2.5	90	3	25
AREVA M5000-116	5.0	116	4	25
Samsung S7.0-171	7.0	171	3	25
AMSC wt10000dd SeaTitan	10.0	190	4	30

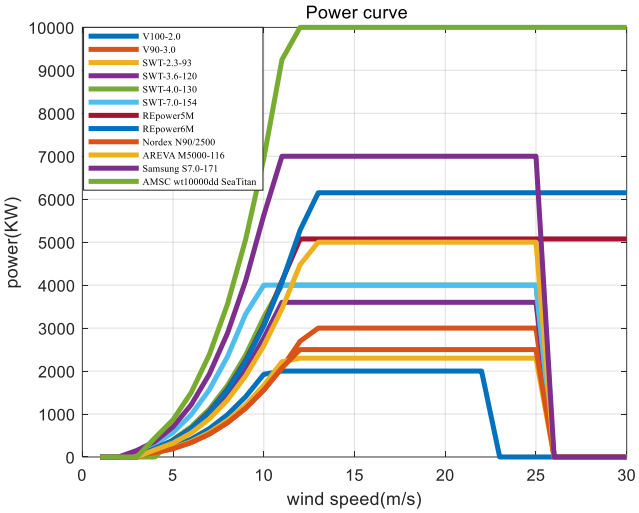

Fig. 7. Power curve for different wind turbines

In addition, capacity factors for different wind turbines at different sites are calculated. All sites and wind turbines are assessed. It can be concluded in Fig. 8 that the selected sites at O16, O17 and O19 show higher capacity (>45%) in the selected wind turbines according to Sant'Anna de Sousa Gomes et al. (2019), and sites with the highest and lowest capacity factors are O16 and O6, respectively.

It can be found from Fig. 8, that the SWT-7.0-154 performs to the best in terms of potential wind energy production, closely followed by V100-2.0. The wind turbine selected in this study is SWT-7.0-154 as it presented the highest performance of wind energy extraction among the selected turbines. It presents maximum use of the wind turbine and higher constancy of energy production throughout the year(Sant'Anna de Sousa Gomes et al., 2019).

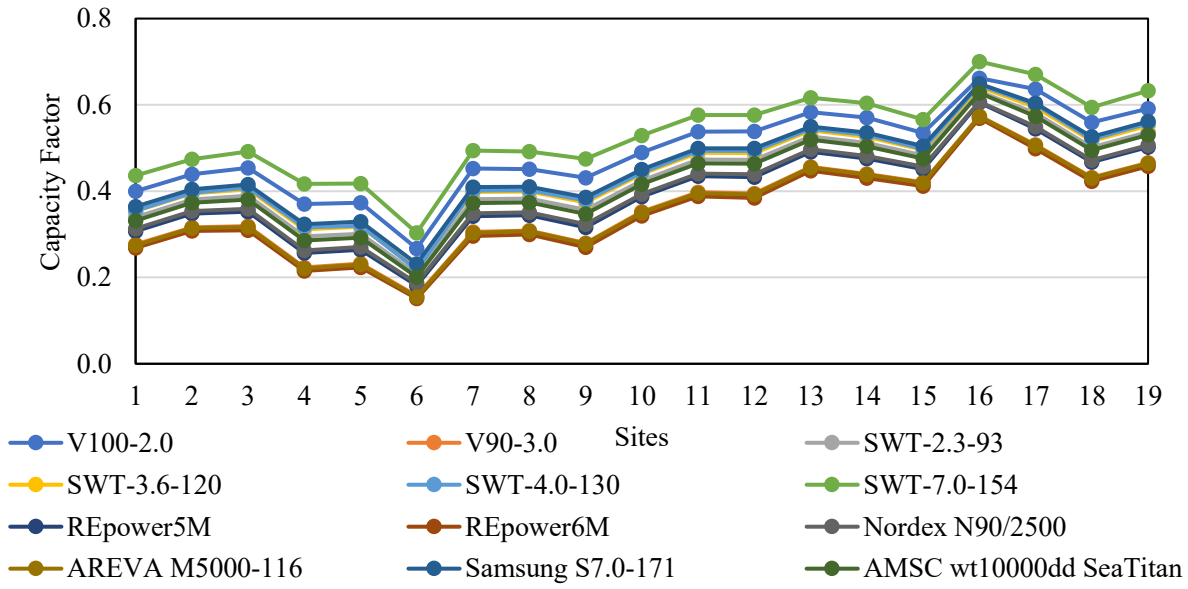

Fig. 8. Capacity factors for different wind turbines at different sites

The total annual energy production in different sites for different wind turbines are calculated from Eq. (3) and shown in Table 3. According to Table 3, the selected site with the highest energy potential is O16 and the lowest energy potential is presented at site O6. Among all analyzed wind turbines, AMSC wt10000dd SeaTitan and V100-2.0 show the highest and lowest energy output, respectively.

Table 3. Total annual energy production of the selected wind turbines at different sites (MWh)

Point ID	V100-2.0	V90-3.0	SWT-2.3-93	SWT-3.6-120	SWT-4.0-130	SWT-7.0-154	REpower5M	REpower6M	Nordex N90/2500	AREVA M5000-116	Samsung S7.0-171	AMSC wt10000ddSeaTitan
O1	7.01	7.27	6.84	11.16	12.42	26.73	13.64	14.46	6.85	12.02	22.32	29.06
O2	7.69	8.31	7.67	12.44	13.88	29.08	15.46	16.60	7.74	13.77	24.80	32.68
O3	7.95	8.37	7.84	12.76	14.30	30.16	15.67	16.68	7.86	13.87	25.46	33.35
O4	6.49	5.87	5.94	9.84	11.06	25.58	11.40	11.58	5.75	9.70	19.86	25.03
O5	6.54	6.09	6.08	10.02	11.21	25.62	11.74	12.03	5.92	10.08	20.18	25.62
O6	4.68	4.14	4.19	7.00	7.64	18.61	8.05	8.15	4.09	6.79	14.21	17.62
O7	7.92	8.03	7.69	12.55	14.07	30.29	15.20	15.94	7.63	13.29	25.11	32.62
O8	7.90	8.12	7.71	12.58	14.10	30.16	15.31	16.13	7.68	13.45	25.14	32.77
O9	7.55	7.35	7.20	11.80	13.25	29.11	14.06	14.56	7.08	12.18	23.67	30.44
O10	8.57	9.25	8.55	13.87	15.52	32.41	17.22	18.48	8.61	15.35	27.61	36.45
O11	9.42	10.45	9.53	15.41	17.29	35.34	19.32	20.89	9.65	17.34	30.61	40.71
O12	9.44	10.36	9.52	15.41	17.29	35.36	19.24	20.69	9.62	17.20	30.62	40.63
O13	10.22	11.99	10.61	17.05	19.09	37.82	21.85	24.08	10.88	19.92	33.73	45.46
O14	10.00	11.56	10.31	16.59	18.59	37.05	21.15	23.17	10.55	19.19	32.86	44.15
O15	9.36	11.05	9.73	15.63	17.44	34.71	20.06	22.20	10.01	18.34	30.94	41.66
O16	11.60	15.09	12.71	20.23	22.61	42.95	26.92	30.67	13.30	25.10	39.80	54.97
O17	11.15	13.34	11.70	18.75	21.04	41.12	24.23	26.86	12.04	22.18	37.05	50.26
O18	9.79	11.34	10.11	16.27	18.22	36.44	20.77	22.79	10.34	18.83	32.24	43.34
O19	10.36	12.24	10.83	17.40	19.52	38.79	22.32	24.66	11.09	20.34	34.43	46.48

Based on the method mentioned above, the WPD, CF, RLO CV, MVI, OM, EWS, EWH, RC, DC and WD are shown in Table 4. According to the table, there are the highest energy potential, extreme wind speed and rate of change, but the lowest accessibility and Coefficient of Variation, at O16. Moreover, O12 performs well in terms of the long-term change for the lowest rate of change of five decades.

Table 4. The values at different sites based on various criteria.

Point ID	WPD(W/m^2)	DC(Km)	CF	RLO	CV	MVI	EWS(m/s)	EWH(m)	ROC	OM	WD(m)
O1	431.23	48.00	0.4359	0.47	2.78	1.02	17.10	1.70	-1.93	0.98	20.00
O2	527.88	47.00	0.4742	0.50	2.69	1.09	18.32	2.48	-1.98	0.96	54.00
O3	519.67	49.20	0.4918	0.53	2.63	0.87	18.44	2.82	-4.22	0.95	39.50
O4	308.94	45.50	0.4172	0.48	2.81	0.59	14.25	2.16	-3.05	0.95	55.00
O5	322.96	7.00	0.4179	0.46	2.83	1.15	14.64	2.45	-2.54	0.94	56.80
O6	210.22	12.80	0.3035	0.32	2.72	1.23	12.94	3.13	-1.78	0.86	57.20
O7	451.62	19.50	0.4940	0.54	2.52	1.14	16.41	3.63	-2.59	0.81	56.00
O8	470.29	49.80	0.4918	0.53	2.79	1.12	16.80	2.95	-2.56	0.88	30.00
O9	402.28	48.30	0.4747	0.52	2.63	0.93	15.73	2.69	-2.11	0.92	30.00
O10	571.35	48.80	0.5286	0.57	2.55	1.17	17.93	2.98	-2.48	0.89	40.00
O11	670.79	49.00	0.5764	0.62	2.40	1.25	18.72	3.38	-0.90	0.83	45.50
O12	627.24	47.00	0.5766	0.62	2.35	1.13	17.70	3.34	-0.39	0.84	55.20
O13	819.74	46.50	0.6168	0.65	2.21	1.24	19.26	3.45	-1.13	0.82	57.70
O14	763.94	49.50	0.6042	0.64	2.20	1.25	18.82	3.39	-1.32	0.84	46.20
O15	787.24	47.50	0.5660	0.59	2.23	1.54	19.62	3.54	-2.97	0.82	29.20
O16	1489.2	41.70	0.7004	0.73	2.00	1.33	23.14	4.04	-6.65	0.73	58.20
O17	976.6	49.40	0.6706	0.71	2.16	1.02	20.42	3.87	-4.82	0.76	41.50
O18	801.54	46.60	0.5942	0.63	2.44	1.04	19.92	3.75	-3.99	0.81	36.00
O19	984.98	46.10	0.6325	0.68	2.52	0.96	22.01	4.20	-4.63	0.77	46.50

The normalized values of the considered criteria and the expectation values are shown in Table 5. This table illustrates the expectation values at different sites. O16 is the most appropriate wind energy extraction location for the wind turbine SWT-7.0-154 considering all criteria. The second choices are O12 and O17. The most suitable location based on this scenario is in line with the results based on the scenarios (Zheng et al., 2018; Costoya et al., 2020; Astariz and Iglesias, 2016; Ferrari et al., 2020). It is interesting to notice that the most suitable location is near the wind farms under construction in Fujian (https://www.4coffshore.com/). It indicates the proposed method provides a tool to decide the suitability of sites by considering different criteria. Therefore, the suggestions for future offshore wind power development should be considered near Hong Kong based on the novel suggested approach. However, the wind turbine

and site selection should not be limited with the above-considered criteria, and other factors such as national and local development policies, electricity demand, etc., may affect the location and wind turbine selection for the installment of a wind farm.

Table 5. The values at different sites based on various criteria after normalized.

Point ID	WPD	DC	CF	RLO	COV	MVI	EWS	EWH	ROC	OM	WD	F
O1	0.29	0.15	0.62	0.64	0.72	0.58	0.76	1.00	0.20	1.00	1.00	0.56
O2	0.35	0.15	0.68	0.68	0.74	0.54	0.71	0.69	0.20	0.98	0.37	0.53
O3	0.35	0.14	0.70	0.73	0.76	0.68	0.70	0.60	0.09	0.97	0.51	0.53
O4	0.21	0.15	0.60	0.66	0.71	1.00	0.91	0.79	0.13	0.97	0.36	0.51
O5	0.22	1.00	0.60	0.63	0.71	0.51	0.88	0.69	0.15	0.96	0.35	0.59
O6	0.14	0.55	0.43	0.44	0.74	0.48	1.00	0.54	0.22	0.88	0.35	0.47
O7	0.30	0.36	0.71	0.74	0.79	0.52	0.79	0.47	0.15	0.83	0.36	0.53
O8	0.32	0.14	0.70	0.73	0.72	0.53	0.77	0.58	0.15	0.90	0.67	0.53
O9	0.27	0.14	0.68	0.71	0.76	0.63	0.82	0.63	0.18	0.94	0.67	0.54
O10	0.38	0.14	0.76	0.78	0.78	0.50	0.72	0.57	0.16	0.91	0.50	0.55
O11	0.45	0.14	0.82	0.85	0.83	0.47	0.69	0.50	0.43	0.85	0.44	0.59
O12	0.42	0.15	0.82	0.85	0.85	0.52	0.73	0.51	1.00	0.86	0.36	0.63
O13	0.55	0.15	0.88	0.89	0.90	0.48	0.67	0.49	0.35	0.84	0.35	0.61
O14	0.51	0.14	0.86	0.88	0.91	0.47	0.69	0.50	0.30	0.86	0.43	0.60
O15	0.53	0.15	0.81	0.81	0.90	0.38	0.66	0.48	0.13	0.84	0.68	0.58
O16	1.00	0.17	1.00	1.00	1.00	0.44	0.56	0.42	0.06	0.74	0.34	0.69
O17	0.66	0.14	0.96	0.97	0.93	0.58	0.63	0.44	0.08	0.78	0.48	0.63
O18	0.54	0.15	0.85	0.86	0.82	0.57	0.65	0.45	0.10	0.83	0.56	0.59
O19	0.66	0.15	0.90	0.93	0.79	0.61	0.59	0.40	0.08	0.79	0.43	0.61

4. Summary and Conclusion

The offshore wind resources were investigated in the South China Sea based on the 55-yearly wind reanalysis dataset developed by the JMA, and a novel suggested approach was proposed to detect the most suitable location for wind turbines installation considering energy potential (WPD, CF, and RLO), stability (MVI and CV), RC, extreme condition (EWS and EWH), OM,

DC and WD.

The results showed that wind energy resource is abundant in the South China Sea. The relatively abundant areas of wind energy resource are mainly in Taiwan Strait and the nearshore northern of Luzon Strait. However, it shows low intra-annual variability of wind resource in the northwest of Taiwan, high variation can be found in Luzon Strait and Central South China Sea.

Long-term change in five decades (from 1961 and 2010) of the offshore wind resource in the South China Sea were analyzed, and the results indicated that there were no noticeable change in most of domain but a slight decrease in Taiwan Strait. Decadal changes were investigated and a remarkable reduction of the wind power density can be observed over the second (1971-1980) decade.

Moreover, 12 wind turbines with different characteristics and 19 sites in the nearshore areas of the South China Sea were selected, and a novel suggested approach considering above-mentioned factors was proposed to detect the most suitable site and wind turbine. The results showed that the most suitable site and wind turbine are O16 (around Fujian) and SWT-7.0-154, respectively. Moreover, the suggestions for future offshore wind power development should be considered near Hong Kong based on the suggested approach, considering that there have been wind farms under construction in Fujian. The average annual output of wind turbine SWT-7.0-154 in the coasts of Hong Kong is 35.36 MWh.

The suggestions for future work in offshore wind resources should investigate economic feasibility, topography conditions and environmental impacts to develop offshore wind farm project in the south coasts of China.

Acknowledgement

This research has been conducted under the grant No. Skhl1807 supported by State Key Laboratory of Hydraulics and Mountain River Engineering, Sichuan University, and the grant from NSFC (51879237). Part of this work has been supported by the Hakubi Center for Advanced Research at Kyoto University, and JSPS Grants-in-Aid for Scientific Research

(KAKENHI), grant No. 20K04705, supported by the Ministry of Education, Culture, Sports, Science, and Technology of Japan (MEXT). The authors are thankful to Japan Meteorological Agency (JMA) for providing JRA-55 dataset.

List of References

Astariz, S., Iglesias, G., 2016. Selecting optimum locations for co-located wave and wind energy farms. Part I: The Co-Location Feasibility index. Energy Conversion and Management 122, 589–598. https://doi.org/10.1016/j.enconman.2016.05.079

Aymen Chaouachib, Catalin Felix Covriga,∗, M.A., 2017. Multi-criteria selection of offshore wind farms Case study for the Baltic States.pdf.

Chou, J.S., Tu, W.T., 2011. Failure analysis and risk management of a collapsed large wind turbine tower. Engineering Failure Analysis 18, 295–313. https://doi.org/10.1016/j.engfailanal.2010.09.008

Costoya, X., deCastro, M., Carvalho, D., Gómez-Gesteira, M., 2020. On the suitability of offshore wind energy resource in the United States of America for the 21st century, Applied Energy. https://doi.org/10.1016/j.apenergy.2020.114537

Dong, S., Gong, Y., Wang, Z., Incecik, A., 2019. Wind and wave energy resources assessment around the Yangtze River Delta. Ocean Engineering 182, 75–89. https://doi.org/https://doi.org/10.1016/j.oceaneng.2019.04.030

Emeksiz, C., Demirci, B., 2019. The determination of offshore wind energy potential of Turkey by using novelty hybrid site selection method. Sustainable Energy Technologies and Assessments 36, 100562. https://doi.org/10.1016/j.seta.2019.100562

Esteban, M.D., Diez, J.J., López, J.S., Negro, V., 2011. Why offshore wind energy? Renewable Energy 36, 444–450. https://doi.org/10.1016/j.renene.2010.07.009

Ferrari, F., Besio, G., Cassola, F., Mazzino, A., 2020. Optimized wind and wave energy resource assessment and offshore exploitability in the Mediterranean Sea. Energy 190, 116447. https://doi.org/10.1016/j.energy.2019.116447

Gallagher, S., Tiron, R., Whelan, E., Gleeson, E., Dias, F., McGrath, R., 2016. The nearshore wind and wave energy potential of Ireland: A high resolution assessment of availability and accessibility. Renewable Energy 88, 494–516. https://doi.org/10.1016/j.renene.2015.11.010

He, J., Chan, P.W., Li, Q., Lee, C.W., 2020. Spatiotemporal analysis of offshore wind field characteristics and energy potential in Hong Kong. Energy 201, 117622. https://doi.org/10.1016/j.energy.2020.117622

Hong, L., Möller, B., 2011. Offshore wind energy potential in China: Under technical, spatial and economic constraints. Energy 36, 4482–4491. https://doi.org/10.1016/j.energy.2011.03.071

Hsu, 1994. Hsu Marine_Power_Law_Wind_Profile 1994.Pdf. American Meteorological Society.

Kamranzad, B., Lin, P., Wen, Y., 2020. Sustainability of wave energy resources in the South

China Sea based on five decades of changing climate. Energy 210, 118604. https://doi.org/10.1016/j.energy.2020.118604

Karamichailidou, D., Kaloutsa, V., Alexandridis, A., 2020. Jo ur na l P re of. Renewable Energy. https://doi.org/10.1016/j.renene.2020.10.020

Kim, J.Y., Oh, K.Y., Kang, K.S., Lee, J.S., 2013. Site selection of offshore wind farms around the Korean Peninsula through economic evaluation. Renewable Energy 54, 189–195. https://doi.org/10.1016/j.renene.2012.08.026

KOBAYASHI, S., OTA, Y., HARADA, Y., EBITA, A., MORIYA, M., ONODA, H., ONOGI, K., KAMAHORI, H., KOBAYASHI, C., ENDO, H., MIYAOKA, K., TAKAHASHI, K., 2015. The JRA-55 Reanalysis: General Specifications and Basic Characteristics. Journal of the Meteorological Society of Japan. Ser. II 93, 5–48. https://doi.org/10.2151/jmsj.2015-001

Lavidas, G., 2020. Selection index for Wave Energy Deployments (SIWED): A near-deterministic index for wave energy converters. Energy 196, 117131. https://doi.org/10.1016/j.energy.2020.117131

Nie, B., Li, J., 2018. Technical potential assessment of offshore wind energy over shallow continent shelf along China coast. Renewable Energy 128, 391–399. https://doi.org/10.1016/j.renene.2018.05.081

O'Connor, M., Lewis, T., Dalton, G., 2013. Weather window analysis of Irish west coast wave data with relevance to operations & maintenance of marine renewables. Renewable Energy 52, 57–66. https://doi.org/10.1016/j.renene.2012.10.021

Sant'Anna de Sousa Gomes, M., Faulstich de Paiva, J.M., Aparecida da Silva Moris, V., Nunes, A.O., 2019. Proposal of a methodology to use offshore wind energy on the southeast coast of Brazil. Energy 185, 327–336. https://doi.org/10.1016/j.energy.2019.07.057

Shu, Z.R., Li, Q.S., Chan, P.W., 2015. Investigation of offshore wind energy potential in Hong Kong based on Weibull distribution function. Applied Energy 156, 362–373. https://doi.org/10.1016/j.apenergy.2015.07.027

Silva, A.R., Pimenta, F.M., Assireu, A.T., Spyrides, M.H.C., 2016. Complementarity of Brazils hydro and offshore wind power. Renewable and Sustainable Energy Reviews 56, 413–427. https://doi.org/10.1016/j.rser.2015.11.045

Wan, Y., Fan, C., Dai, Y., Li, L., Sun, W., Zhou, P., Qu, X., 2018. Assessment of the Joint Development Potential of Wave and Wind Energy in the South China Sea. Energies 11. https://doi.org/10.3390/en11020398

Wang, L., Ning, J., Li, Y., Du, F., 2020. Responses of hyperiid (Amphipoda) communities to monsoon reversal in the central South China Sea. Progress in Oceanography 102440. https://doi.org/10.1016/j.pocean.2020.102440

Wang, Z., Duan, C., Dong, S., 2018. Long-term wind and wave energy resource assessment in the South China sea based on 30-year hindcast data. Ocean Engineering 163, 58–75. https://doi.org/https://doi.org/10.1016/j.oceaneng.2018.05.070

WINDPOWER, 2020, n.d. No Title [WWW Document]. URL https://www.thewindpower.net/store_actor_en.php?id_type=5

Wu, Y., Tao, Y., Zhang, B., Wang, S., Xu, C., Zhou, J., 2020. A decision framework of offshore wind power station site selection using a PROMETHEE method under

intuitionistic fuzzy environment: A case in China. Ocean and Coastal Management 184, 105016. https://doi.org/10.1016/j.ocecoaman.2019.105016

Zheng, C., Pan, J., Li, J., 2013. Assessing the China Sea wind energy and wave energy resources from 1988 to 2009. Ocean Engineering 65, 39–48. https://doi.org/https://doi.org/10.1016/j.oceaneng.2013.03.006

Zheng, C. wei, Xiao, Z. niu, Peng, Y. hua, Li, C. yin, Du, Z. bo, 2018. Rezoning global offshore wind energy resources. Renewable Energy 129, 1–11. https://doi.org/10.1016/j.renene.2018.05.090

Zhou, J., Wu, Z., Jin, X., Zhao, D., Cao, Z., Guan, W., 2018. Observations and analysis of giant sand wave fields on the Taiwan Banks, northern South China Sea. Marine Geology 406, 132–141. https://doi.org/10.1016/j.margeo.2018.09.015